



Published in final edited form as:

J Allergy Clin Immunol. 2020 November ; 146(5): 1204–1208.e6. doi:10.1016/j.jaci.2020.06.032.

A novel *STING1* variant causes a recessive form of STING-associated vasculopathy with onset in infancy (SAVI)

Bin Lin, PhD^{a,*}, Roberta Berard, MD, MSc^{b,*}, Abdulrahman Al Rasheed, MD, MBBS, CAPB^{c,*}, Buthaina Aladba, MD, MBBS, CAPB^{d,*}, Philip J. Kranzusch, PhD^{e,f}, Maggie Henderlight, BS^g, Alexi Grom, MD^g, Dana Kahle, BS^a, Sofia Torreggiani, MD^a, Alexander G. Aue^a, Jacob Mitchell, BS^a, Adriana A. de Jesus, MD, PhD^a, Grant S. Schulert, MD, PhD^{g,‡}, Raphaela Goldbach-Mansky, MD, MHS^{a,‡}

^aTranslational Autoinflammatory Diseases Section, Laboratory of Clinical Immunology and Microbiology, National Institute of Allergy and Infectious Diseases, Bethesda, Md

^bDepartment of Pediatrics, Western University, London, Ontario, Canada

^cDivision of Rheumatology, Pediatric Department, King Abdullah Specialized Children Hospital, King Abdulaziz Medical City, Riyadh, Saudi Arabia

^dSidra Medical and Research Center, Department of Pediatric Medicine, Division of Rheumatology, Doha, Qatar

^eDepartment of Microbiology, Harvard Medical School, Boston, Mass

^fDepartment of Cancer Immunology & Virology, Dana-Farber Cancer Institute, Boston, Mass

^gCincinnati Children's Hospital Medical Center and Department of Pediatrics, University of Cincinnati College of Medicine, Cincinnati, Ohio.

To the Editor:

Stimulator of interferon response genes (*STING*) encoded by stimulator of interferon response cGAMP interactor 1 (*STING1*), previously known as transmembrane protein 173 (*TMEM173*) is an important pattern recognition receptor that detects microbial dinucleotides and functions as an adaptor molecule in the cytosolic DNA sensing pathway that binds 2'3'-cyclic GMP-AMP (cGAMP), which is generated when cytosolic DNA activates cyclic GMP-AMP synthase (cGAS).^{1,2} *STING* activation stimulates the induction of type I interferons, which activate interferon responses. Gain-of-function (GOF) variants in *STING1* lead to autoactivation without ligand binding and cause a rare autoinflammatory disease named *STING*-associated vasculopathy with onset in infancy (SAVI) (Online Mendelian Inheritance in Man catalog no. 615934).^{3,4} Patients with SAVI present in

This is an open access article under the CC BY-NC-ND license (<http://creativecommons.org/licenses/by-nc-nd/3.0/>).

goldbacr@mail.nih.gov.

*These authors share co-first authorship.

‡These authors contributed equally to this work.

Disclosure of potential conflict of interest: R. Goldbach-Mansky has received grant support from SOBI, Regeneron, Novartis, and Eli Lilly. The rest of the authors declare that they have no relevant conflicts of interest.

infancy with the following symptoms: recurrent fevers; cold-induced skin vasculitis that can progress to tissue loss and amputation of fingers and toes; and/or interstitial lung disease, which is the main cause of the mortality that often occurs before patients reach adulthood. So far, all reported cases of SAVI have been caused by autosomal dominant variants, with most of them occurring *de novo*.

We have identified 6 patients from 4 unrelated families, all of whom are of Arabic ethnicity and harbor pathogenic *STING1* variants that are disease causing only in homozygosity. The patients had clinical disease suggestive of SAVI and were enrolled into institutional review board–approved protocols, including the National Institutes of Health natural history protocol (NCT02974595).

Patient 1, the index patient, presented at 4 weeks of age with a cough and failure to thrive, as well as with a maculopapular violaceous rash with a livedoid appearance (Fig 1, A and B). A chest computed tomography scan showed diffuse bilateral parenchymal opacities. His lung disease progressed despite steroid therapy and short-term treatment with the JAK inhibitor tofacitinib, and he died of respiratory failure at 5 months of age. His older brother (patient 2) died at 18 months of age with chronic cough and failure to thrive. Although genetic testing was not performed, the clinical manifestations and similarities of patient 2 to those of his younger brother strongly suggest that he had SAVI. Patient 3 presented at 3 months of age with recurrent fever, erythematous rash, cough, and dyspnea, ultimately progressing to oxygen dependence. He had a chest computed tomography scan with results consistent with interstitial lung disease and a lung biopsy specimen that showed chronic interstitial pneumonitis with intraalveolar hemorrhage. He is currently taking the JAK inhibitor ruxolitinib. His brother, patient 4, had respiratory symptoms starting at the age of 6 months; he was diagnosed with SAVI at the age of 15 months and was initially treated with steroids, after which baricitinib (a selective JAK1/2 inhibitor) was added to his treatment regimen. Patient 5 presented at the age of 2 months with cough, tachypnea, and recurrent lung infections; she was diagnosed with chronic aspiration pneumonia and had a laryngeal cleft that was repaired at the age of 4.5 years. Because of her lung disease (Fig 1, E), she has required supplemental oxygen since the age of 7 months and bilevel positive airway pressure support while sleeping since the second year of life, when digital clubbing was noticed. She developed pulmonary hypertension by the age of 4 years. At the age of 5 she developed polyarthritis, an erythematous rash over the soles of her feet and clubbing. She began taking baricitinib at the age of 7 years; there was clinical improvement, but her oxygen dependence continued. Patient 6 presented at the age of 8 months with a history of persistent tachypnea and failure to thrive, polyarthritis, intermittent vasculitic rashes, and clubbing (Fig 1, C and D). All of the parents and siblings were asymptomatic with normal inflammatory markers. Additional clinical and laboratory information is available in Table E1 (in this article's Online Repository at www.jacionline.org).

Patients 1, 3, and 4 underwent targeted sequencing of *STING1*, whereas whole exome sequencing was performed on families 3 and 4. Sequencing of all patients revealed a homozygous *STING1* (NM_198282) variant c.841C>T, p.Arg281Trp, p.R281W (Fig 1, F). This variant was present in heterozygosity in only 2 of 282,822 alleles reported in gnomAD (gnomad.broadinstitute.org) and is predicted to be damaging by PolyPhen-2 and

deleterious by the scale-invariant feature transform algorithm (SIFT), and it has a Combined Annotation-Dependent Depletion (CADD)-PHRED-scaled score of 26.4. This variant has not been reported previously in patients with SAVI (<https://infervers.umai-montpellier.fr>). All of the parents, as well as several of the unaffected siblings, were heterozygous carriers of this variant (Fig 1, F). A variant affecting the same amino acid residue but mutated to a glutamine (c.842G>A, p.Arg281Gln, p.R281Q) has previously been described to cause an autosomal dominant form of SAVI⁵ (Fig 1, G).

A strikingly high interferon response gene signature and systemic inflammation in patients with SAVI has led to their designation as having an autoinflammatory interferonopathy.⁶ A standardized interferon response gene score was elevated only in patients who were homozygous for the p.R281W variant and who had clinical disease, and not in the siblings and parents who were heterozygous carriers of the variant or in healthy controls (Fig 1, H).

Transfection of HEK293T cells with the *STING1* construct containing the R281W mutation led to activation of *IFNB1* luciferase reporter without ligand binding (see Fig E1 in this article's Online Repository at www.jacionline.org), indicating that p.R281W is a pathogenic GOF variant. The mutant remained responsive to cGAMP (see Fig E1), suggesting no effect on ligand binding.

Disease-causing SAVI variants³ cluster in 2 areas. The cryoelectron microscopy structure model of STING⁷ has mapped the class 1 variants, p.N154S, p.V155M, and p.V147L to the connector helix loop (Fig 1, G) which controls a cGAMP ligand-induced 180° rotation of the ligand-binding area of the STING dimer that induces polymerization and activation. The class 3 variants, including p.R281Q, p.R284G⁵ and p.R284S,⁸ are located at the polymerization interface⁷ (Fig 1, G) and have been postulated to bind a C-terminal tail that might prevent polymerization and autoactivation.⁹

Concordant with previous reports, we hypothesized that the p.R281W variant confers a GOF that is weaker than the heterozygous SAVI variants. To test this possibility, we transfected HEK293T cells with either wild-type or mutant STING constructs including R281W at increasing concentrations and assessed *IFNB1* reporter activity (Fig 2, A). At equal transfection efficiency, consistent with the homozygosity requirement at this location, R281W mutant constructs exhibited lower autoactivation than R281Q constructs did but were similar to mutant constructs with the pathogenic V155M variant. This suggests differential autoactivation thresholds for disease-causing class 1 variants at the connector helix loop (ie, V155M) versus class 3 variants at the polymer interface (ie, R281 and R284). In line with this hypothesis, pathogenic variants at the class 3 residues that cause disease in heterozygosity, including R281Q, R284S, and R284G, are all more autoactivating than V155M in the transfection model (Fig 2, A and B), with R284S, R284G, and G158A constituting the top 3 autoactivating SAVI variants (Fig 2, B).

Although class 1 disease-causing SAVI variants are GOF variants, mutating these residues into charged amino acids (eg, V155R³ and G158E⁸) leads to loss of function, likely through destabilizing the STING dimer structure. In contrast, none of the 6 different amino acid mutations at position R281 caused loss of function (Fig 2, B [*green labels*]). In fact, all of

the mutations except for R281A, which is similar to the wild type, led to autoactivation. Maintenance of a positive charge at residue R281 (by mutating into lysine [K] or histidine [H]) was insufficient to keep STING inactive at the basal state. Moreover, mutations into hydrophobic amino acids such as tryptophan (W), leucine (L), or methionine (M), or into negatively charged amino acids (including glutamic acid [E]), cause autoactivation (Fig 2, A and B). The autoactivation was not due to differential protein expression in the transfection assay (see Fig E2 in this article's Online Repository at www.jacionline.org). The R281 and R284 mutations that were assessed remained responsive to cGAMP stimulation (Fig 2, B and see Fig E1), indicating no effect on ligand binding. The broad autoactivation of the R281 and R284 mutations was consistent with the model of polymer interface binding to an inhibitor to suppress STING autoactivation.⁹ Although this potential inhibitor is not addressed in the 180° rotation model of the connector helix loop mutations, it is quite likely that the 180° rotation also leads to loss of inhibitor binding on the polymer interface, thus allowing side-by-side packing. Our data thus suggest a possible common mechanism to reconcile the 2 previously reported structural models (Fig 2, C and see also the Discussion section for detailed description of the model shown in Fig E3 in this article's Online Repository at www.jacionline.org), which is supported by similar superactivating mutations in both the connector helix loop (G158A) and the polymer interface (R281E, R284G, and R284S).

In summary, we have reported 6 patients from 4 unrelated families with recessively inherited *STING1* variants and characteristic clinical features of SAVI. Our data support the notion that the disease-causing homozygous p.R281W variant causes GOF but is weaker in activating STING than the previously reported heterozygous variants, and it requires biallelic mutations to constitutively activate STING. We have demonstrated a critical role of residue R281 in maintaining STING in an inactive state, likely without affecting dimer conformation. Our data unveil limitations of the current structural models that cannot explain the superactivating potential of the R281 and R284 mutations and raise questions as to whether class 3 residues represent an autoinhibitory domain or a binding site for an external inhibitor of STING. Considering the critical function of R281 and the nearby region, novel therapeutic options may arise from high-throughput screens of drugs that bind to this area and inhibit polymerization.

Acknowledgments

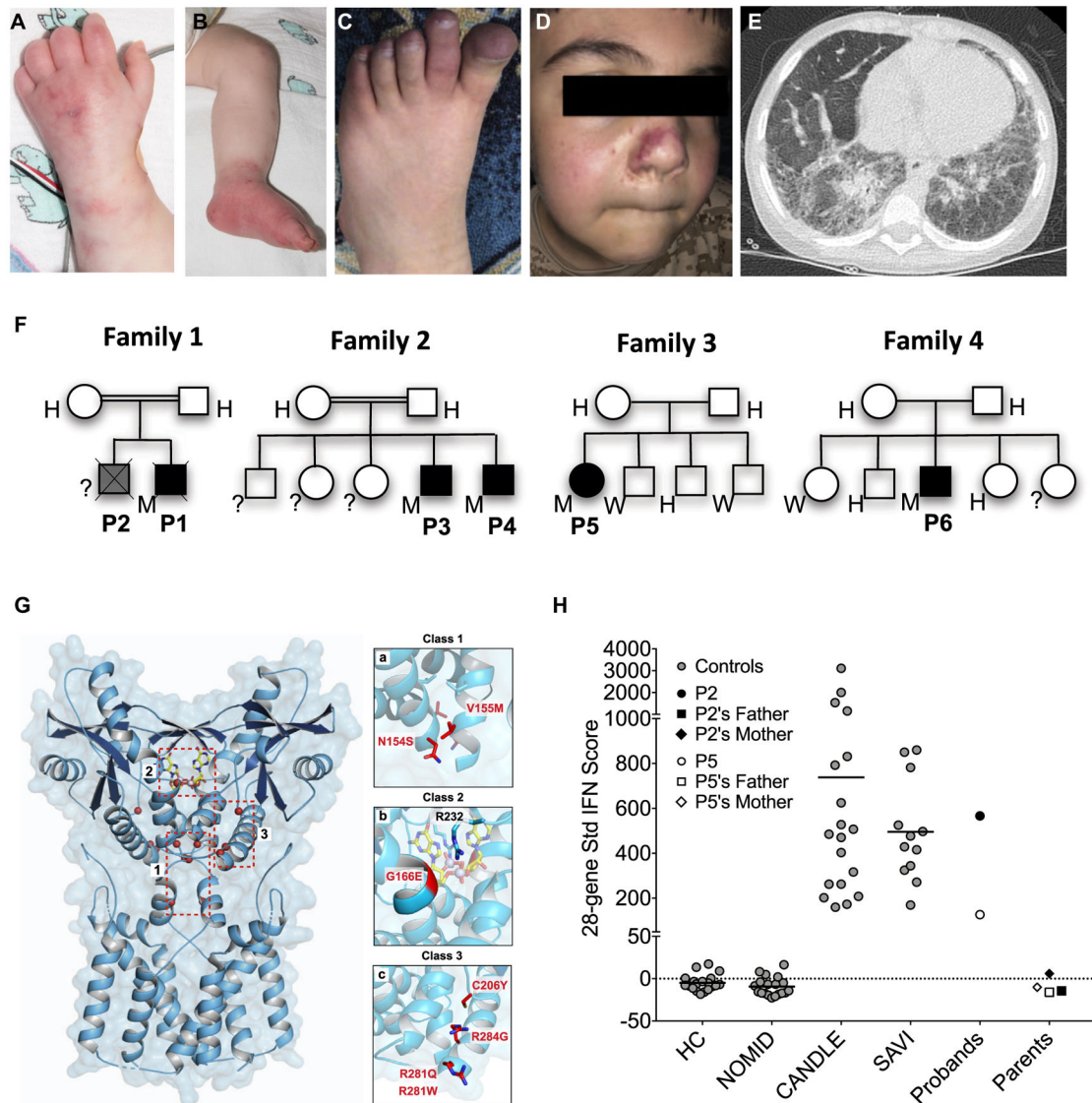
We thank the patients and their families for participating in this study.

This research was supported by the Intramural Research Program of the National Institutes of Health (NIH), National Institute of Allergy and Infectious Diseases (to R.G.-M.); grant K08 AR072075 (to G.S.S.) from NIH, National Institute of Arthritis, Musculoskeletal and Skin Diseases; and an Academic Research and Clinical (ARC) grant from Cincinnati Children's Research Foundation (to A.G. and G.S.S.).

REFERENCES

1. Ishikawa H, Ma Z, Barber GN. STING regulates intracellular DNA-mediated, type I interferon-dependent innate immunity. *Nature*2009;461:788–92. [PubMed: 19776740]
2. Ablasser A, Chen ZJ. cGAS in action: Expanding roles in immunity and inflammation. *Science*2019;363.

3. Liu Y, Jesus AA, Marrero B, Yang D, Ramsey SE, Sanchez GAM, et al. Activated STING in a vascular and pulmonary syndrome. *N Engl J Med* 2014;371:507–18. [PubMed: 25029335]
4. Jeremiah N, Neven B, Gentili M, Callebaut I, Maschalidi S, Stolzenberg MC, et al. Inherited STING-activating mutation underlies a familial inflammatory syndrome with lupus-like manifestations. *J Clin Invest* 2014;124:5516–20. [PubMed: 25401470]
5. Melki I, Rose Y, Ugenti C, Van Eyck L, Fremond ML, Kitabayashi N, et al. Disease-associated mutations identify a novel region in human STING necessary for the control of type I interferon signaling. *J Allergy Clin Immunol* 2017;140: 543–52.e5. [PubMed: 28087229]
6. Kim H, de Jesus AA, Brooks SR, Liu Y, Huang Y, VanTries R, et al. Development of a validated interferon score using nanostring technology. *J Interferon Cytokine Res* 2018;38:171–85. [PubMed: 29638206]
7. Shang G, Zhang C, Chen ZJ, Bai XC, Zhang X. Cryo-EM structures of STING reveal its mechanism of activation by cyclic GMP-AMP. *Nature* 2019;567:389–93. [PubMed: 30842659]
8. Konno H, Chinn IK, Hong D, Orange JS, Lupski JR, Mendoza A, et al. Pro-inflammation associated with a gain-of-function mutation (R284S) in the innate immune sensor STING. *Cell Rep* 2018;23:1112–23. [PubMed: 29694889]
9. Ergun SL, Fernandez D, Weiss TM, Li L. STING polymer structure reveals mechanisms for activation, hyperactivation, and inhibition. *Cell* 2019;178: 290–301.e10. [PubMed: 31230712]

**FIG 1.**

Homozygous *STING1* variant p.R281W causes SAVI. **A-E**, Clinical images showing typical cutaneous features of vasculopathy for patient 1 (P1) (**A** and **B**) and P6 (**C** and **D**), as well as a chest computed tomography scan (**E**) demonstrating reticulonodular densities throughout (P5). **F**, Family trees. **G**, Location of p.R281W and other disease-causing SAVI mutations in the cryoelectron microscopy structure model of STING. Highlighted are previously reported class 1 mutations in the connector helix loop, class 2 mutation in the cGAMP binding pocket, and class 3 mutations on a surface-exposed region of STING dimer. **H**, Interferon (IFN) scores of p.R281W homozygous patients and their parents compared with those of healthy controls (HCs) or patients with neonatal-onset multisystem inflammatory disease (NOMID), chronic atypical neutrophilic dermatosis with lipodystrophy and elevated temperature (CANDLE), or SAVI with heterozygous GOF *STING1* mutations. *H*, Heterozygous; *M*, homozygous; *Std*, standard; *W*, wild type.

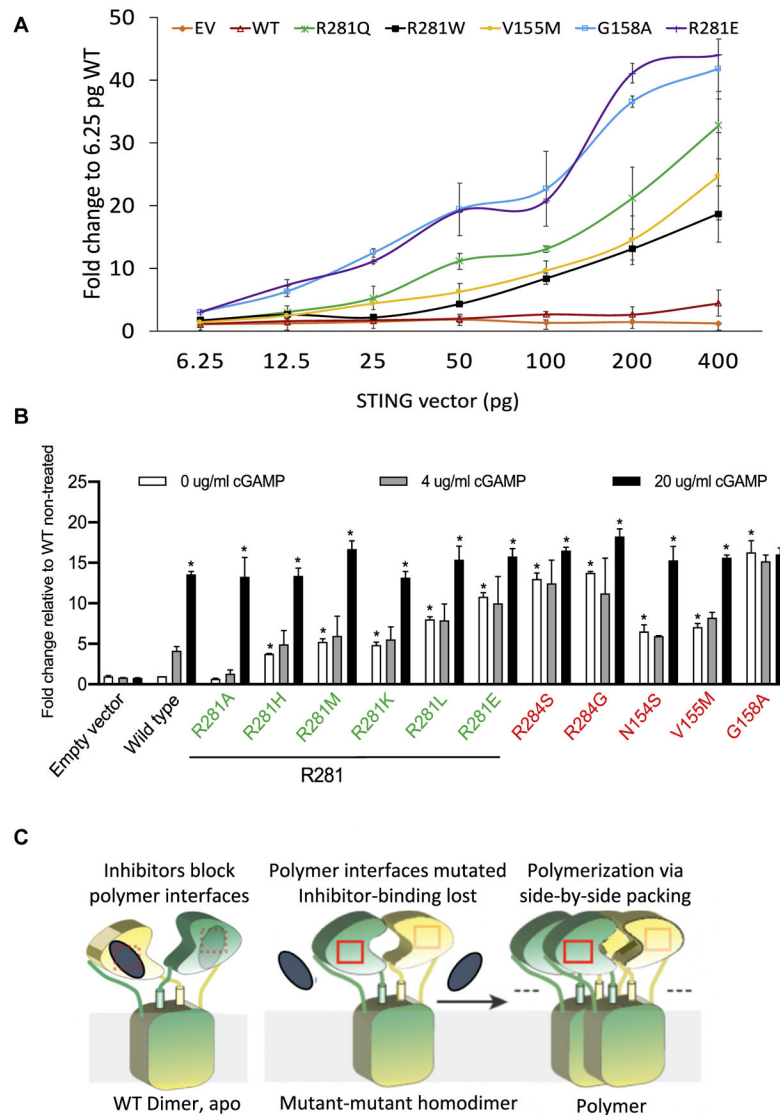


FIG 2. Multiple random *STING1* mutations at p.R281 lead to strong autoactivation. **A**, *IFNβ1* reporter activation by R281W and other *STING* constructs transfected into HEK293T cells at increasing concentrations. **B**, R281 mutations led to strong *STING* autoactivation, as measured by *IFNβ1* reporter activation in HEK293T cells. In particular, R281E was superactivating, comparable to the most activating mutation G158A *in vitro*. Quantities of 50 pg of various *STING* constructs were transfected into 30,000 cells. cGAMP at various concentrations was used to activate *STING*. SAVI-causing mutations are labeled in red, and other R281 mutations are labeled in green. *An asterisk above the white bar designating 0 μg/mL of cGAMP indicates a significant change ($P < .0001$) compared with the wild-type (WT) nontreated cells (indicated by the white bar), as determined by the use of ordinary 1-way ANOVA (Dunnett multiple comparisons tests). An asterisk above the black bar designating 20 μg/mL of cGAMP indicates a significant change ($P < .003$) of cells treated with 20 μg/mL of cGAMP compared with the respective nontreated cells (indicated by the

respective *white bar*), as determined by the use of 2-way ANOVA (Bonferroni multiple comparisons tests). Data are presented as means \pm SDs of duplicates. Similar results were obtained in independent experiments. **C**, A reconciled model to explain autoactivation of polymer interface mutations. The 2 subunits of STING dimer are shown in yellow and green. Polymer interfaces are indicated by *red boxes*. Inhibitors are shown as *gray ellipses*. The model assumes a putative inhibitor that is bound to the polymer interface and is unable to bind in patients with disease-causing mutation in either the connector helix loop region or in the polymer interface. For the full model and a detailed description, see also Fig E3. *EV*, Empty vector; *WT*, wild-type. *Modified with permission from Shang et al.*^{E1}